Inorg. Chem. **2002**, *41*, 1930–1939

Metallonitrosyl Fragment as Electron Acceptor: Intramolecular Charge Transfer, Long Range Electronic Coupling, and Electrophilic Reactivity in the *trans*-$[NCRu(py)_4(CN)Ru(py)_4NO]^{3+}$ Ion

Federico Roncaroli, Luis M. Baraldo,* Leonardo D. Slep,* and José A. Olabe*

Departamento de Química Inorgánica, Analítica y Química Física, Inquimae, Facultad de Ciencias Exactas y Naturales, Universidad de Buenos Aires, Pabellón 2, Ciudad Universitaria, C1428EHA Buenos Aires, República Argentina

Received September 20, 2001

The new complex *trans*-$[NCRu(py)_4(CN)Ru(py)_4NO](PF_6)_3$ (**I**) was synthesized. In acetonitrile solution, **I** shows an intense visible band (555 nm, $\epsilon = 5800\ M^{-1}\ cm^{-1}$) and other absorptions below 350 nm, associated with $d_\pi \rightarrow \pi^*_{py}$ and $\pi_{py} \rightarrow \pi^*_{py}$ transitions. The visible band is presently assigned as a donor–acceptor charge transfer (DACT) transition from the remote Ru(II) to the delocalized $\{Ru^{II}–NO^+\}$ moiety. Photoinduced release of NO is observed upon irradiation at the DACT band. Application of the Hush model reveals strong electronic coupling, with $H_{DA} = \sim 2000\ cm^{-1}$. The difference between the optical absorption energy and redox potentials for the donor and acceptor sites ($Ru^{III,II}$, 1.40 V, and NO^+/NO, 0.50 V, vs Ag/AgCl, 3 M KCl, respectively) ($h\nu - \Delta E_{red}$) is 1.33 eV, a large value which probably relates to the significant changes in distances and angles for the Ru–N–O moiety upon reduction. UV–vis absorptions, IR frequencies, and redox potentials are solvent-dependent. Controlled potential reduction (of NO^+) and oxidation (of Ru(II) associated with the dicyano-chromophore) of **I** afford stable species, $[NCRu^{II}(py)_4(CN)Ru(py)_4NO]^{2+}$ ($\mathbf{I}_{red}$) and $[NCRu^{III}(py)_4(CN)Ru(py)_4NO]^{4+}$ ($\mathbf{I}_{ox}$), respectively, which are characterized by UV–vis and IR spectroscopies. $\mathbf{I}_{red}$ shows an EPR spectrum characteristic of $\{Ru(II)–NO^\bullet\}$ complexes. Compound **I** is electrophilically reactive in aqueous solution above pH 5: values of the equilibrium constant for the reaction $[NCRu(py)_4(CN)Ru(py)_4NO]^{3+} + 2\ OH^- \rightleftarrows [NCRu(py)_4(CN)Ru(py)_4NO_2]^+ + H_2O$, $K = 3.2 \pm 1.4 \times 10^{15}\ M^{-2}$, and of the rate constant for the nucleophilic addition of OH^-, $k = 9.2 \pm 0.2 \times 10^3\ M^{-1}\ s^{-1}$(25 °C, $I = 1$ M), are obtained, with $\Delta H^\ddagger = 90.7 \pm 3.8\ kJ\ mol^{-1}$ and $\Delta S^\ddagger = 135 \pm 13\ J\ K^{-1}\ mol^{-1}$. The oxidized complex, $\mathbf{I}_{ox}$, shows an enhanced electrophilic reactivity toward OH^-. This addition reaction is followed by irreversible processes, which most probably lead to disproportionation of bound nitrite and other products.

Introduction

An increasing effort is nowadays directed to synthesize compounds in which relevant spectroscopic and reactivity properties can be put under precise control. Recently, we focused our efforts in the study of the reactivity changes of coordinated ligands upon variations on the oxidation state of metals located at extended distances. We studied the chemical electrophilic reactivity of bound nitrosyl in the $[(NH_3)_5Ru^{II,III}(NC)Os(CN)_4NO]^{0,1+}$ ions and found a five-order of magnitude increase in the rate constant for OH^- addition upon oxidation of the distant ruthenium center from the II to the III state.[1] The cyano bridge seems to play a key role in the metal−metal electronic coupling responsible for the above-mentioned property.[2] Cyano-bridged polynuclear metal complexes have, in fact, received considerable attention over recent years,[3] restimulated by studies on mixed-valent compounds, as well as on photoinduced electron- and energy-transfer processes.[4]

* Authors to whom correspondence should be addressed. E-mail: baraldo@q1.fcen.uba.ar (L.M.B.); slep@q1.fcen.uba.ar (L.D.S.); olabe@q1.fcen.uba.ar (J.A.O.). Fax: 5411-4576-3341 (J.A.O.).

(1) Forlano, P.; Parise, A. R.; Olabe, J. A. *Inorg. Chem.* **1998**, *37*, 6406.
(2) (a) Scandola, F.; Argazzi, R.; Bignozzi, C. A.; Chiorboli, C.; Indelli, M. T.; Rampi, M. A. *Coord. Chem. Rev.* **1993**, *125*, 283. (b) Watzy, M. A.; Endicott, J. F.; Song, Z.; Lei, Y.; Macatangay, A. V. *Inorg. Chem.* **1996**, *35*, 3463. (c) Macatangay, A. V.; Endicott, J, F. *Inorg. Chem.* **2000**, *39*, 437. (d) Watson, D. F.; Bocarsly, A. B. *Coord. Chem. Rev.* **2001**, *211*, 177. (e) Pfennig, B. W.; Fritchman, V. A.; Hayman, K. A. *Inorg. Chem.* **2001**, *40*, 255. (f) Wang, C.; Mohney, B. K.; Williams, R. D.; Petrov, V.; Hupp, J. T.; Walker, G. C. *J. Am. Chem. Soc.* **1998**, *120*, 5848. (g) Karki, L.; Hupp, J. T. *J. Am. Chem. Soc.* **1997**, *119*, 4070. (h) Vance, F. W.; Karki, L.; Reigle, J. K.; Hupp, J. T.; Ratner, M. A. *J. Phys. Chem. A* **1998**, *102*, 8320. (i) Bublitz, G. U.; Laidlaw, W. M.; Denning, R. G.; Boxer, S. G. *J. Am. Chem. Soc.* **1998**, *120*, 6068.

10.1021/ic0109896 CCC: $22.00
Published on Web 03/12/2002

We considered it valuable to synthesize new *trans*-cyano-bridged complexes, on the basis of recent work with *trans*-$\{Ru(py)_4\}^{2+}$ centers, which proved to be highly stable (unlike the $\{Ru^{II}(bpy)_2\}$ analogues) and may act as nonchromophoric spacers in oligometallic structures.[5,6] The advantages of synthesizing complexes with *trans* bridging units, instead of the more commonly found *cis* ones, as with *cis*-$\{Ru(bpy)_2\}^{2+}$-based complexes, has been emphasized.[7] The *trans* geometry yields structurally well-defined assemblies (without potential structural isomerism), appropriate to study long-range processes.

The nitrosyl ligand appeared as a good candidate for probing the changes of reactivity when bound to the new oligomeric structures. The studies with bound nitrosyl deserve special attention in the context of modern coordination chemistry,[8] particularly the redox interconversions, which are known to be important in fundamental processes in NO biochemistry, such as transport, uptake, and delivery in the biological fluids.[9] As a typical noninnocent ligand, nitrosyl can act mainly as a diamagnetic, strongly π-accepting[8] NO^+ or as the paramagnetic, one-electron reduced molecule, NO.[10] The presence of the two-electron reduced species, HNO, has also been demonstrated in several bound systems.[11] In this context, the synthesis of the new dinuclear compound, *trans*-$[NCRu^{II}(py)_4(CN)Ru^{II}(py)_4NO](PF_6)_3$, was conceived as a tool for better understanding the factors that effectively control the reactivity of NO^+, particularly its behavior as an electrophile[12] and its ability to dissociate from the relevant metal centers upon changing redox state. The possibility of variation of the adjacent coligands as well as the distant metal fragment was a part of the synthetic strategy designed for expanding the still limited set of mononuclear complexes where structure−reactivity studies have been made available. In addition, the presence of an exposed cyanide ligand in the *trans*-position to the nitrosyl sets the basis for further coordination of additional metal fragments, to obtain potential molecular wires.

Experimental Section

Materials. Acetonitrile (AcN, Merck) was distilled under argon after refluxing for 12 h over CaH_2. Tetra-*n*-butylammonium hexafluorophosphate, $TBAPF_6$ (Aldrich), was recrystallized from ethanol. NaCl was p.a. grade (Merck). Decamethylferrocene (Aldrich) was used as provided. The precursor compounds $[RuCl_2(py)_4]$, *trans*-$[Ru(CN)_2(py)_4]\cdot H_2O$, and *trans*-$[RuCl(py)_4(NO)](PF_6)_2$ were prepared according to literature procedures.[5,13]

Water for the electrochemical experiments was deionized and distilled after refluxing for 6 h over alkaline $KMnO_4$. All other solvents and solid reagents were obtained commercially and used without further purification. Elemental analyses were carried out by H. Kolbe in Mülheim an der Ruhr, Germany.

Preparation of *trans*-$[NC(py)_4Ru(CN)Ru(py)_4(NO)](PF_6)_3$ (I). A 0.30 g portion of *trans*-$[Cl(py)_4Ru(NC)Ru(py)_4(CN)]PF_6$ (0.28 mmols)[7] and 1.00 g of $NaNO_2$ (14.5 mmols) were suspended in 400 mL of deaerated water. The mixture was stirred in the dark for 48 h under an Ar atmosphere. The clear solution was then concentrated to 25 mL, and ~1 mL of an NH_4PF_6 saturated water solution was added to afford a yellow solid, which was collected by filtration.

Purification was performed by ion-exchange chromatography (Dowex 50W X2, 100−200 mesh, H^+ form, $l = 20$ cm, $d = 2.5$ cm) as follows: the crude product was dissolved in 50 mL of 0.1 M HCl yielding a deep violet solution, which was seeded in the column and eluted with HCl 1:4. The first major violet fraction was collected and precipitated with ~20 mL of the NH_4PF_6 solution. The obtained solid was repurified following the same procedure, taking special care to collect exclusively the first fraction with absorption maximum at 518 nm. Addition of saturated NH_4PF_6 solution yielded a violet solid, which was collected by filtration and dried in vacuo (yield 0.150 g, 40%). Anal. Calcd for $[NCRu(py)_4(CN)Ru(py)_4NO](PF_6)_3$: C, 37.32; H, 2.98; N, 11.40. Found: C, 37.16; H, 3.10; N, 11.27. NMR: δ_H (CD_3CN) 8.32 (4 H, t, $H^4 \times 4$), 8.15 (16H, m, $H^{2,6}$ $H^{2'6'} \times 4$), 7.87 (4H, t, $H^{4'} \times 4$), 7.59 (8H, t,$H^{3'5'} \times 4$), 7.16 (8H, t, $H^{3,5} \times 4$); δ_C (CD_3CN) 158.32 (8C, $C^{3.5} \times 4$), 155.01 (8C, $C^{3',5'} \times 4$), 144.19 (4C, $C^4 \times 4$), 138.46 (4C, $C^4 \times 4$), 129.94 (8C, $C^{2,6} \times 4$), 126.64 (8C, $C^{2'6'} \times 4$). Despite several attempts, we were not able to obtain single crystals suitable for X-ray diffraction analysis.

Instrumentation and General Procedures. Ultraviolet−visible spectra were recorded with a diode-array instrument, HP 8453, using an RC 6 Lauda thermostat and 1-cm quartz cells. Infrared spectra were obtained using either Nicolet 510P or Perkin-Elmer 2000 FTIR spectrometers; solution spectra were obtained using a cell with CaF_2 windows of 3 cm ∅ and a 0.05 mm spacer. NMR spectra were

(3) (a) Dunbar, K. R.; Heintz, R. A. *Prog. Inorg. Chem*. **1997**, *45*, 283. (b) Vahrenkamp, H.; Geiss, A.; Richardson, G. N. *J. Chem. Soc., Dalton Trans.* **1997**, 3643. (c) Wu, Y.; Pfennig, B. W.; Sharp, S. L.; Ludwig, D. R.; Warren, C. J.; Vicenzi, E. P.; Bocarsly, A. B. *Coord. Chem. Rev.* **1997**, 159, 245. (d) Doorn, S. K.; Blackbourn, R. L.; Johnson, C. S.; Hupp, J. T. *Electrochim. Acta* **1991**, *36*, 1775.

(4) (a) Pfennig, B. W.; Lockard, J. V.; Bocarsly, A. B. *Inorg. Chem.* **1999**, *38*, 2941. (b) Pfennig, B. W.; Cohen, J. L.; Sosnowski, I.; Novotny, N. M.; Ho, D. M. *Inorg. Chem.* **1999**, *38*, 606. (c) Pfennig, B. W.; Goertz, J. K.; Wolff, D. W.; Cohen, J. L. *Inorg. Chem.* **1998**, *37*, 2608. (d) Wang, C.; Mohney, B. K.; Akhremitchev, B. B.; Walker, G. C. *J. Phys. Chem. A* **2000**, *104*, 4314. (e) Richardson, G. N.; Brand, U.; Vahrenkamp, H. *Inorg. Chem.* **1999**, *38*, 3070. (f) Zhu, N.; Vahrenkamp, H. *Chem. Ber./Recl.* **1997**, *130*, 1241. (g) Kunkely, H.; Vogler, A. *Inorg. Chim. Acta* **1997**, *254*, 195. (h) Argazzi, R.; Bignozzi, C. A.; Heimer, T. A.; Meyer, G. J. *Inorg. Chem*. **1997**, *36*, 2. (i) Thompson, D. W.; Schoonover, J. R.; Meyer, T. J.; Argazzi, R.; Bignozzi, C. A. *J. Chem. Soc., Dalton Trans*. **1999**, 3729. (j) Forlano, P.; Parise, A. R.; Videla, M.; Olabe, J. A. *Inorg. Chem.* **1997**, *36*, 5642. (k) Bernhardt, P. V.; Macpherson, B. P.; Martínez, M. *Inorg. Chem.* **2000**, *39*, 5203.

(5) Coe, B. J.; Meyer, T. J.; White, P. S. *Inorg. Chem*. **1995**, *34*, 593.

(6) (a) Bottomley, F.; Mukaida, M. *J. Chem. Soc., Dalton Trans*. **1982**, 1933. (b) Kimura, T.; Sakurai, T.; Shima, M.; Togano, T.; Mukaida, M.; Nomura, T. *Inorg. Chim. Acta* **1983**, *69*, 135.

(7) Coe, B. J.; Meyer, T. J.; White, P. S. *Inorg. Chem*. **1995**, *34*, 3600.

(8) Richter-Addo, G. B.; Legzdins, P. *Metal Nitrosyls*; Oxford University Press: New York, 1992.

(9) (a) *Methods in Nitric Oxide Research*; Feelisch, M.; Stamler J. S., Eds.; J. Wiley & Sons: Chichester, 1996. (b) Butler, A. R.; Glidewell, C. *Chem. Soc. Rev.* **1987**, *16*, 61. (c) Clarke, M. J.; Gaul, J. B. *Struct. Bonding (Berlin)* **1993**, *81*, 147.

(10) (a) Cheney, R. P.; Simic, M. G.; Hoffman, M. Z.; Taub, I. A.; Asmus, K. D. *Inorg. Chem.* **1977**, *16*, 2187. (b) van Voorst, J. D. W.; Hemmerich, P. *J. Chem. Phys.* **1966**, *45*, 3914. (c) Nast, R.; Schmidt, J. *Angew. Chem., Int. Ed. Engl.* **1969**, *8*, 383. (d) Butler, A. R.; Calsy-Harrison, A. M.; Glidewell, C. *Polyhedron*, **1988**, *7*, 1197.

(11) (a) Southern, J. S.; Hillhouse, G. L. *J. Am. Chem. Soc.* **1997**, *119*, 12406. (b) Wilson, R. D.; Ibers, J. A. *Inorg. Chem*. **1979**, *18*, 336. (c) Lin, R.; Farmer, P. J. *J. Am. Chem. Soc*. **2000**, *122*, 2393. (d) Sellman, D.; Gottschalk-Gaudig, T.; Hausinger, D.; Heinemann, F. W.; Hess, B. A. *Chem. Eur. J.* **2001**, *7*, 2099.

(12) (a) Bottomley, F. In *Reactions of Coordinated Ligands*; Braterman, P. S., Ed.; Plenum: New York, 1985; Vol. 2, p 115. (b) Bottomley, F. *Acc. Chem. Res*. **1978**, *11*, 158.

(13) Evans, I. P.; Spencer, A.; Wilkinson, G. *J. Chem. Soc., Dalton Trans.* **1973**, 204.

measured with a Bruker AM-500 spectrometer. The resonance Raman (RR) spectrum was measured in AcN using a rotating cell (path length 1-cm) to prevent photodegradation. The cell was purged with N_2 and hermetically sealed. For excitation, the 568-nm line of a cw Kr-ion laser (Coherent 302) was used, with power of ~40 mW at the sample. The scattered light (90°) was focused onto the entrance slit of a double monochromator (ISA, U1000) working as a spectrograph and equipped with a liquid nitrogen cooled CCD camera. The spectral bandwidth was 4 cm^{-1}, and the increment per data point, 0.53 cm^{-1}. The total accumulation time of the RR spectra was 20 s. The spectra are the average of at least 3 independent measurements. Background was removed by polynomial subtraction. Electrochemical measurements were made using a PAR model 273A potentiostat, in aqueous and AcN solutions, with 0.1 M NaCl or $TBAPF_6$ as supporting electrolytes, respectively. A glassy carbon disk (d = 3 mm) was used as the working electrode, with Pt and Ag/AgCl, 3 M KCl, as counter and reference electrodes, respectively. In AcN, a silver wire was used, with decamethylferrocene as an internal reference. The presently reported potentials refer to the Ag/AgCl, 3 M KCl reference electrode (0.21 V vs NHE). The spectroelectrochemical and coulometric experiments were done under argon in 0.1 M $TBAPF_6$ AcN solutions. The *trans*-$[NCRu^{II}(py)_4(CN)Ru^{II}(py)_4NO]^{3+}$ complex was alternatively reduced and oxidized at −20 °C under controlled potential conditions. These procedures were repeated several times without decomposition, as proved by UV−vis and IR spectroscopies. Samples prepared in this way were transferred via syringe for EPR analysis. The infrared spectroelectrochemical experiments were performed using a three-electrode OTTLE cell. For the UV−vis spectroelectrochemistry, a specially modified 1-cm path length quartz cuvette attached to a 5-mL glass container was used. The whole setup was purged with Ar and thermostatised (Lauda RL6 CP cryostat). Electrolysis was performed over a platinum net. A second platinum net separated by a frit glass was used as a counter electrode, and $Ag/AgNO_3$ (AcN) was used as a reference. X-band EPR spectra were determined with a Bruker ESP 300E spectrometer equipped with a helium flow cryostat (Oxford Instruments ESR 910). The spectra were recorded at 9.45 GHz, 10 μW power, 100 kHz modulation frequency, and 10.0 G modulation amplitude. The one-electron oxidized product of *trans*-$[Ru(CN)_2(py)_4]$ and the one-electron reduced product of *trans*-$[RuCl(py)_4(NO)]^{2+}$ were prepared and characterized in a similar way, providing valuable information for the spectral assignments in the diruthenium compounds.

Spectroelectrochemical experiments with **I** in the UV−vis region (reduction and oxidation) were also done in aqueous solutions (see Table 1 for details).

Nucleophilic Addition to Bound Nitrosyl. We performed equilibrium and kinetic studies of OH^- addition into **I**. The solutions for the equilibrium measurements were prepared in the pH range 4.50−6.62, by mixing 1.00 mL of a 4.0 × 10^{-4} M solution of **I** with 4.00 mL of a buffer solution (acetate or phosphate, final I = 1 M, NaCl). All the solutions were equilibrated in the dark at 25.0 ± 0.1 °C for at least 12 h before recording the spectra. A multiwavelength global analysis of the absorbance versus pH data[14] accounted for only two colored species. Application of the chemical model described by eq 1 afforded the equilibrium constant and the spectra of the species present in solution.

$$[NCRu(py)_4CNRu(py)_4NO]^{3+} + 2OH^- \rightleftarrows [NCRu(py)_4CNRu(py)_4NO_2]^{+} + H_2O \quad (1)$$

The temporal evolution of the reaction was monitored spectrophotometrically following the disappearance of **I** at 518 nm. Solutions in the pH range 6.75−8.15 were prepared by mixing 1 mL of a ~5 × 10^{-5} M solution of **I** with 2 mL of a phosphate buffer solution (final I = 1 M, NaCl). Temperature variation in the range 20.0−40.0 ± 0.1 °C afforded the activation parameters.

Photolysis of *trans*-$[NCRu^{II}(py)_4(CN)Ru^{II}(py)_4NO]^{3+}$. Aqueous and AcN solutions of **I** were irradiated with a UV filtered halogen lamp (150 W). The products were tested through UV−vis, IR, and electrochemical measurements. In aqueous solution, the release of NO was detected with a specific amiNO-100 electrode (Innovative Instruments, Inc.). Fast decomposition of **I** was achieved by using unfiltered radiation.

Results

Electrochemistry. Figure 1 shows a typical cyclic voltammogram (CV) of **I** in AcN. Two reversible processes at $E_{1/2}$ = 0.50 and 1.40 V are observed, which correspond to a one-electron reduction and one-electron oxidation of **I**, as indicated by controlled potential coulometry.[15] Table 1 collects the half-wave potentials, including values in aqueous solution. In this case, both waves are shifted to more negative potentials ($E_{1/2}$ = 0.22 and 1.18 V, respectively). The waves are fully reversible in the pH range 0−2. In the pH range 2−6, an anodic scan (square wave voltammetry, SWV) reveals the same waves, but a reductive scan (starting at 1.3 V, with 5 s of equilibration time) triggers the appeareance of new waves, revealing the onset of irreversible chemical reactions following one-electron oxidation. Above pH 9, both redox waves are replaced by new ones at $E_{1/2}$ = 0.83 and 1.20 V. These results suggest that not only **I** but also its oxidized form, $\mathbf{I_{ox}}$, might be reactive toward OH^-. We describe this in more detail in the section devoted to Electrophilic Reactivity.

Electronic Spectra. The visible region of the spectrum of **I** in AcN is dominated by an intense absorption centered at 555 nm (ϵ = 5800 $M^{-1}cm^{-1}$). Figure 2 displays the changes observed in the electronic spectra upon controlled potential conversion to the one-electron reduced ($\mathbf{I_{red}}$) and the one-electron oxidized ($\mathbf{I_{ox}}$) species in the same solvent. Table 1 includes the absorption maxima and molar absorbances for the three redox-linked species. Data for related mononuclear complexes are also included for comparison. The reduction process induces the decay of the 555 nm band and the growth of new bands in the UV region, red-shifted with respect to those of **I** (Figure 2 (top)). The existence of several isosbestic points indicates that side reactions are absent. The total charge related to this conversion accounts for one electron. Chemical reduction under mild conditions using 1 equiv of decamethylferrocene yields the same spectral changes. $\mathbf{I_{red}}$ showed to be stable for hours under anaerobic conditions and can be reoxidized electrochemically or by exposing the solution to air, with total recovery of the characteristic spectrum of **I**. The same holds true for the behavior of the reduced species obtained from $[Ru^{II}Cl(py)_4NO]^{2+}$.

(14) Slep, L. D.; Pollak, S.; Olabe, J. A. *Inorg. Chem.* **1999**, *38*, 4369.
(15) A third irreversible wave at ca. −0.4 V (see Table 1) was also observed when extending the potential sweep range. It is most probably related to an additional one-electron reduction with further ligand labilization.[8,9]

Table 1. UV−Vis, IR, and Electrochemical Results (Acetonitrile and Aqueous Solutions) for the $[NCRu^{II}(py)_4(CN)Ru^{II}(py)_4NO]^{3+}$ Ion (**I**) and Its Reduced $[NCRu^{II}(py)_4(CN)Ru^{II}(py)_4NO]^{2+}$ (**I_{red}**) and Oxidized Forms $[NCRu^{III}(py)_4(CN)Ru^{II}(py)_4NO]^{4+}$ (**I_{ox}**)

	λ_{max} (ϵ),[a] nm (M^{-1} cm^{-1})			ν, cm^{-1}		$E_{1/2}$ (ΔE_p), V[b]	
complex	AcN [c]	H_2O [d]	assignment	AcN [c]	H_2O [d]	AcN	H_2O
I	555 (5800)	518 [e]	$d_\pi \rightarrow \pi^*_{NO}$	2050 vw	2032 vw	1.40 [f] (90)	1.18 [g]
	330 (14300)	317 (14500)	$d_\pi \rightarrow \pi_{py}$ [h]	2001 s	2014 [i] s	0.50 [f] (95)	0.22 [g]
	256sh (20000)	260sh (20000)	$\pi_{py} \rightarrow \pi^*_{py}$ [h]	1976 w		−0.45 [f,j]	−0.39 [j,k]
	237 (27600)	233 (32000)	$d_\pi \rightarrow \pi^*_{py}$ [l]	1917 s	1923 [m] s		
I_{red}	350 (18500)	333 (20200)	$d_\pi \rightarrow \pi^*_{py}$ [h]	2056 [n] s			
	290 (15000)	294 (20300)	$d_\pi \rightarrow \pi^*_{py}$ [l]	2033 sh			
	262 (25000)	262sh (23600)	$\pi_{py} \rightarrow \pi^*_{py}$ [l]				
	245 (25700)	239sh (32100)	$\pi_{py} \rightarrow \pi^*_{py}$ [h]	1626 s			
I_{ox}	440 (1020)	532sh (500)	$CN^- \rightarrow d_\pi$	2137 [o] m			
	401 (2600)	440sh (1670)	$CN^- \rightarrow d_\pi$	2120 s			
	329 (3420)	400 (3500)	$CN^- \rightarrow d_\pi$	1952 s			
	295 (4320)	299 (9200)	$CN^- \rightarrow d_\pi$				
	260 (24600)	266sh (25300)	$\pi_{py} \rightarrow \pi^*_{py}$ [h]				
		260 (28800)					
$[Ru(CN)_2(py)_4]$ [p]	374 (22500)		$d_\pi \rightarrow \pi^*_{py}$	2062 s		0.80	
	248 (15500)		$\pi_{py} \rightarrow \pi^*_{py}$				
$[Ru(CN)_2(py)_4]^+$	475 (650)		$CN^- \rightarrow d_\pi$	2108 s			
	377 (1900)		$CN^- \rightarrow d_\pi$				
	258 (21000)		$\pi_{py} \rightarrow \pi^*_{py}$				
$[RuCl(py)_4NO]^{2+}$ [p,q]	450 (150)		$d-d$; $d_\pi \rightarrow \pi^*_{NO}$	1910 s		0.31 (100)	0.10
	258 (15100)		$\pi_{py} \rightarrow \pi^*_{py}$				−0.24
	232 (20000)		$d_\pi \rightarrow \pi^*_{py}$			−0.62	−0.45
$[RuCl(py)_4NO]^+$	377 (730)		$d_\pi \rightarrow \pi^*_{NO}$	1610 s			
	290 (11500)		$d_\pi \rightarrow \pi^*_{py}$				
	261 (14500)		$\pi_{py} \rightarrow \pi^*_{py}$				

[a] Bands below 230 nm are not reported. [b] Against Ag/AgCl, 3 M KCl. [c] See text for experimental details in AcN. [d] Electroreduction in aqueous solution was performed at $E_{appl} = 0$ V vs Ag/AgCl, over a platinum net, $I = 0.1$ M, HCl. The electrooxidation was performed at $E_{appl} = 1.4$ V, in 1 M HNO_3 for the absorptions above 300 nm, and 0.01 M for those below 300 nm. [e] 1 M HCl. [f] CV, 0.02 V/s, in 0.1 M $TBAPF_6$. [g] SWV, 60 Hz, 1 M HNO_3. [h] Corresponding to the dicyano chromophore. [i] In KBr disk, 2011 cm^{-1}. [j] Irreversible wave. [k] SWV, 60 Hz, 0.01 M HCl, 1 M NaCl. [l] Corresponding to the NO-containing chromophore. [m] In KBr disk, 1917 cm^{-1}. [n] Spectroelectrochemical reduction. [o] Spectroelectrochemical oxidation. [p] Ref 5. [q] The bands at 258 and 232 nm were assigned to $d_\pi \rightarrow \pi^*_{py}$ and $\pi_{py} \rightarrow \pi^*_{py}$, respectively, in ref 5.

Figure 2 (bottom) shows the electrooxidation experiment. A decay of the UV−vis bands of **I** is also observed, with new bands for **I_{ox}** appearing at 440, 401, 329, 295, and 260 nm. The same considerations about isosbestic points and total charge hold true in this case. **I_{ox}** was stable in AcN solution, and **I** was recovered quantitatively by electrochemical reduction. Remarkably, **I_{ox}** proved to be very reactive toward traces of water in the solvent. This last observation is related to the complications already described in the electrochemical experiments. For these reasons, the characterization of the three redox-related species in aqueous solution was performed in l M or 0.01 M HNO_3 solutions, keeping in mind the onset of electrophilic reactivity. Under these conditions, the redox processes showed an equivalent picture as for AcN. Electrochemical reduction of **I** triggers the complete decay of the band at 518 nm and the appearance of several new bands in the UV region. The electrooxidation experiments, if done at pHs lower than 2, show that **I_{ox}** is also obtained, without attack at the NO^+ site. This is shown by its CV response (identical to the one displayed by **I**) and the replacement of the UV absorptions characteristic of the Ru^{II}−py chromophores by new absorptions in the near-UV−vis

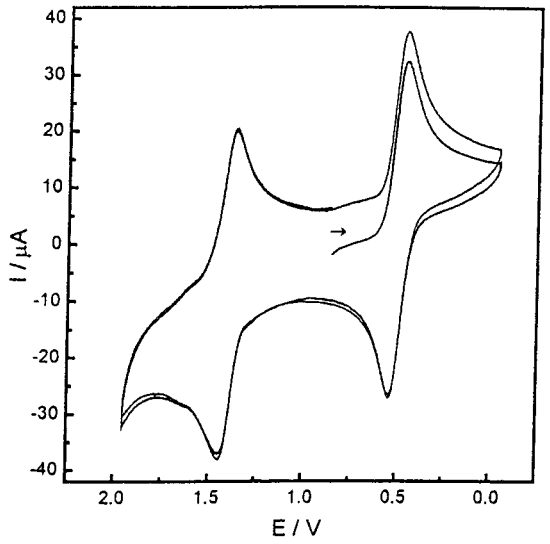

Figure 1. Cyclic voltammogram of $[NCRu(py)_4(CN)Ru(py)_4NO](PF_6)_3$ in acetonitrile solution, 0.1 M $TBAPF_6$, scan rate 20 mV/s, $T = 25$ °C.

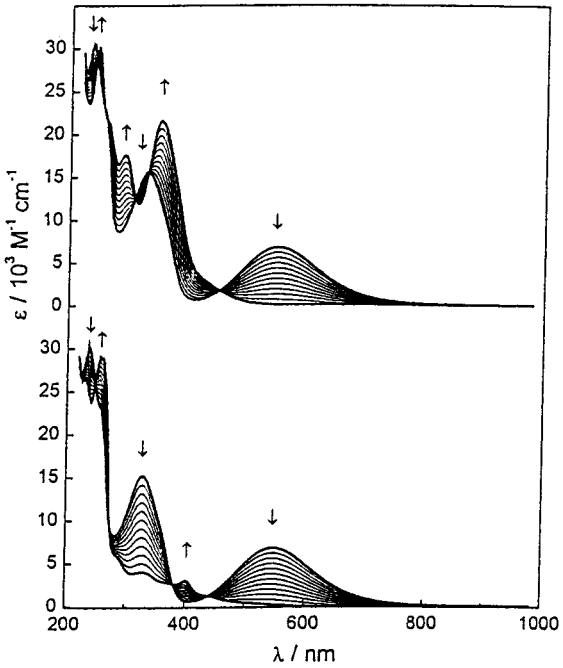

Figure 2. UV−vis spectroelectrochemistry of $[NCRu(py)_4(CN)Ru(py)_4NO](PF_6)_3$ in acetonitrile solution, 0.1 M $TBAPF_6$, $T = -20$ °C. Top: one-electron reduction. Bottom: one-electron oxidation.

region, which we assign as before for the case of AcN solutions. Chemical oxidation of **I** with 1 equiv of Ce(IV) induces similar spectral changes. In both cases, **I** can be recovered electrochemically at $E_{app} = 0.6$ V. In general terms, the energies of the near-UV−vis bands for all the dinuclear species shift to greater energies in water compared to AcN, by ~1300 cm^{-1} (see Table 1, including values for the absorption maxima below 300 nm, which are unshifted in both solvents).

Infrared Spectroscopy. The cyanide and nitrosyl stretching vibrations, ν_{CN} and ν_{NO}, are very sensitive to the redox changes. Figure 3 shows the IR spectrum of **I** in AcN, with signals at 2001 and 1976 cm^{-1} (assigned as ν_{CN}, see below) and 1917 cm^{-1}, corresponding to ν_{NO}. A very weak absorption can also be appreciated at ~2050 cm^{-1}. Upon electrochemical one-electron reduction, ν_{CN} and ν_{NO} shift in opposite directions: the former to 2056 cm^{-1} and the latter to 1626 cm^{-1}. A slight shift of the band at 1612 cm^{-1} (probably associated with pyridine vibrations) to 1609 cm^{-1} is also observed. Chemical reduction using decamethylferrocene or $[RuCl_2(py)_4]$ affords the same spectral features.

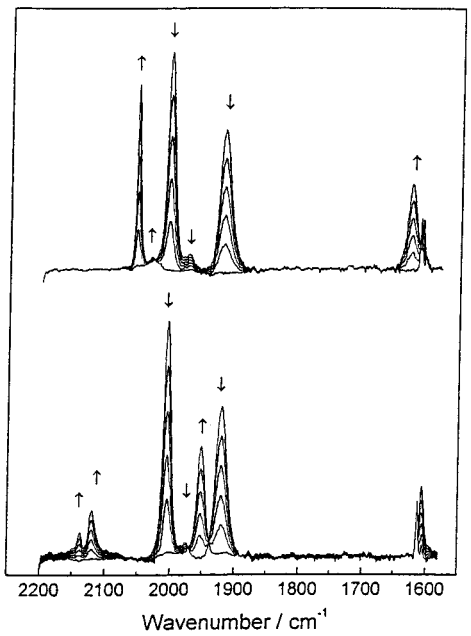

Figure 3. Infrared spectroelectrochemistry of $[NCRu(py)_4(CN)Ru(py)_4NO](PF_6)_3$ in acetonitrile solution, 0.1 M $TBAPF_6$, $T = -20$ °C. Top: one-electron reduction. Bottom: one-electron oxidation.

In the one-electron oxidized product, $\mathbf{I_{ox}}$, new ν_{CN} and ν_{NO} bands develop at 2137, 2120, and 1952 cm^{-1}, respectively. Table 1 collects the vibrational information and includes stretching frequencies obtained in aqueous solution, where all the signals are blue-shifted compared to AcN.

Raman Spectrum of I. A preliminary experiment was performed by irradiating near the maximum of the intense visible band, under resonance conditions. A strong signal appeared at 2000 cm^{-1}, together with a medium-intensity one at 1920 cm^{-1}.

EPR. Figure 4 shows the spectra of $\mathbf{I_{red}}$ and *trans*-$[RuCl(py)_4NO]^+$ at 10 K. The samples were electrogenerated and rapidly frozen in liquid N_2. Also shown are the results of the powder simulation,[16] obtained including hyperfine coupling with one nitrogen nucleus (^{14}N, 99.64% natural abundance, $I = 1$) and using the spin Hamiltonian parameters $\bar{g} = (1.990, 2.024, 1.865)$ and $\bar{A}/10^{-4}$ $cm^{-1} = (31.7, 14.5, 9.1)$ for $\mathbf{I_{red}}$ and $\bar{g} = (1.989, 2.033, 1.874)$ and $\bar{A}/10^{-4}$ $cm^{-1} = (29.7, 14.1, 10.0)$ for *trans*-$[RuCl(py)_4NO]^+$. As will be discussed later, these features agree with other reports on coordinated $NO^{\bullet}$, including ruthenium complexes.[17,18]

(16) Neese, F. Diploma Thesis, University of Konstanz, 1993.
(17) (a) McGarvey, B.; Ferro, A. A.; Tfouni, E.; Bezerra, C. W. B.; Bagatin, I.; Franco, F. F. *Inorg. Chem.* **2000**, *39*, 3577. (b) Lantg, D. R.; Davis, J. A.; Lopes, L. G. F.; Ferro, A. A.; Vasconcellos, L. C. G.; Franco, D. W.; Tfouni, E.; Wieraszko, A.; Clarke, M. J. *Inorg. Chem.* **2000**, *39*, 2294.

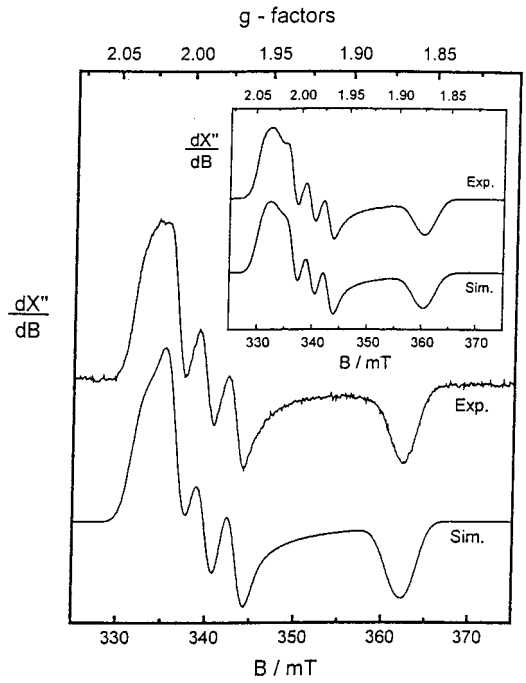

Figure 4. Top: EPR spectrum of electrogenerated $[NCRu(py)_4(CN)Ru(py)_4NO]^{2+}$ in acetonitrile, 0.1 M $TBAPF_6$, at 10 K. Bottom: computer simulated spectrum with the parameters detailed in the text (see results section). Inset: same but for the $[RuCl(py)_4NO]^{+}$ ion.

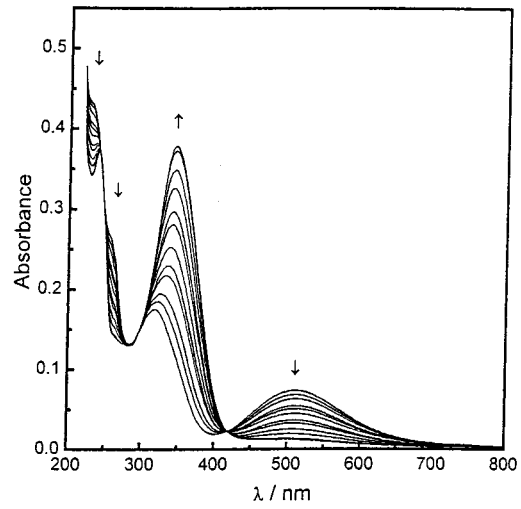

Figure 5. Time evolution of the UV−vis spectra for an aqueous solution of $[NCRu(py)_4CNRu(py)_4NO](PF_6)_3$ (pH 6.77; I = 1 M, NaCl; T = 30 °C). The arrows indicate the changes in band intensities as the reaction proceeds.

Electrophilic Reactivity. Figure 5 shows the consecutive spectra obtained for the reaction of **I** with OH^-, according to eq 1. The consumption of **I** is revealed by the decrease in intensity of the characteristic bands at 233, 255, and 518 nm. The original band at 317 nm shifts to 345 nm, with an increase in intensity. The conversion comprises well-defined isosbestic points in the complete UV−vis region, and the product is stable on the time scale of hours. The equilibrium constant is $K_1 = 3.2 \pm 1.4 \times 10^{15}$ M^{-2} (25 °C, I = 1 M). Equal amounts of the nitrosyl and nitro species are present at pH 6.3. Acidification down to pH 4 quantitatively recovers **I**.

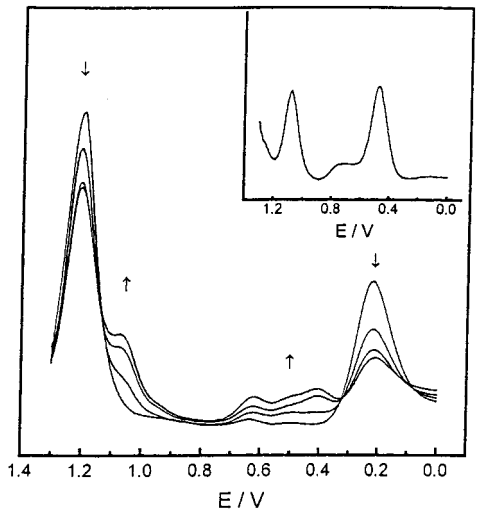

Figure 6. Consecutive SWV scans for the electrooxidation of an aqueous solution of $[NCRu(py)_4(CN)Ru(py)_4NO](PF_6)_3$ at 1.3 V (pH 4.0; I = 1 M, NaCl; T = 25 °C). Each scan was obtained after 15 s of electrolysis. Inset: scan after exhaustive oxidation at the same potential.

The rate law for reaction 1 shows a first-order behavior with respect to the concentrations of OH^- and **I**, with $k_1 = 9.2 \pm 0.2 \times 10^3$ M^{-1} s^{-1} (25 °C, I = 1 M). The activation parameters are $\Delta H^{\ddagger} = 90.7 \pm 3.8$ kJ mol^{-1} and $\Delta S^{\ddagger} = 135 \pm 13$ J K^{-1} mol^{-1}.

The electrochemistry above pH 2 provides some insight on the electrophilic reactivity of $\mathbf{I_{ox}}$. For example, at pH 4.0, after setting the potential at 1.3 V for 15 s, new waves appear at 0.41, 0.49, 0.62, and 1.07 V (Figure 6). Longer oxidation periods increase the intensity of the new waves, while the waves assigned to **I** (0.22 and 1.2 V) decrease. Following exhaustive electrolysis at 1.3 V, the SWV reveals the complete disappearance of **I** and the formation of a new product with waves at 0.47 and 1.07 V, together with minor quantities of other species. Exhaustive reduction at 0.7 or 0.3 V did not recover **I**. The solution reduced at 0.7 V was precipitated with NH_4PF_6, and the solid obtained did not show bands associated with the nitrosyl stretching. The nature of this product is still uncertain, but the evidence clearly suggests that above pH 2 the electrogenerated $\mathbf{I}_{ox}$ is reactive toward nucleophilic attack by OH^-.

Photoreactivity. The complex **I** was photolyzed in aqueous and AcN solutions, the decomposition being faster in the latter case. The UV−vis bands of **I** disappear, and the IR absorptions of the product suggest the presence of Ru(III). In water, at pH 4, the presence of free NO was detected, subsequently to light flashing.

Discussion

Our previous work on dinuclear, cyano-bridged complexes containing the nitrosyl ligand, $[(NH_3)_5Ru^{II,III}(NC)M(CN)_4NO]^{0,1+}$ (M = Fe, Ru, Os),[1] suggested a significant electronic interaction between the metal centers, mediated by cyanide,

(18) Wanner, M.; Scheiring, T.; Kaim, W.; Slep, L. D.; Baraldo, L. M.; Olabe, J. A.; Zális, S.; Baerends, E. J., *Inorg. Chem.* **2001**, *40*, 5704. DFT calculations show that the singly occupied molecular orbital (SOMO) has around 65% of NO character for the pentacyanonitrosyl complexes, with a 25% metal contribution.

as revealed by an intense band ($\epsilon = \sim 4000\ M^{-1}\ cm^{-1}$) in the visible region and significant effects on the electronic structure and electrophilic reactivity of the (formally) NO^+ ligand upon changing the redox state of the *distant* $[Ru(NH_3)_5]$ fragment. Our work showed for the first time that the strongly coupled $\{M-NO\}^6$ moiety (usually considered to contain $M^{II}-NO^+$)[8] might behave as the acceptor component of the overall charge transfer (CT) process promoted by the $[Ru^{II}(NH_3)_5]$ donor fragment. We now succeeded in preparing complex **I**, a system where the geometry of the bridge is clearly defined as *trans* to the nitrosyl ligand. In this way, both ruthenium, the cyano bridge, and the NO^+ ligand lay on the same axis. Two sets of four equivalent pyridines (as revealed by the ^1H and ^{13}C NMR) and a distant exposed cyanide complete the coordination spheres.

Figure 1 shows that complex **I** can undergo reversible one-electron reduction in AcN, leading to the formation of $\mathbf{I_{red}}$. The EPR X-band spectrum of $\mathbf{I_{red}}$ in frozen AcN displayed in Figure 4 is comparable to the one obtained from *trans*-$[RuCl(py)_4NO]^+$. In both cases, the *g* and nitrogen hyperfine coupling tensors are consistent with an unpaired electron in a NO π^* orbital. Although the free $NO^\bullet$ radical does not exhibit an EPR spectrum under normal conditions, coordination to metal centers provides EPR signals which allow for an analysis of the electronic structure. Following previous work,[17,18] we conclude that the EPR signals arise from bound $NO^\bullet$ radicals in which the axial symmetry is removed by coordination. The largest ^{14}N hyperfine component lays along the *x* axis of the *g* tensor, indicating that the unpaired electron is in the π_x orbital of $NO^\bullet$.[18] The large anisotropy in the *g* tensor suggests a bent Ru(II)$-NO^\bullet$ motif.

The IR spectrum of $\mathbf{I_{red}}$ (Figure 3a) also agrees with a nitrosyl-centered reduction: ν_{NO} shifts significantly from 1917 to 1626 cm^{-1}, as found with several reduced nitrosyl-complexes,[19,20] consistent with a decrease in bond order upon reduction. The ν_{CN} values of $\mathbf{I_{red}}$ are around 2050 cm^{-1}, typical of cyanide coordinated to Ru(II) centers.[21] The spectroscopic evidence thus suggests that $\mathbf{I_{red}}$ is best described as $[NCRu^{II}(py)_4(CN)Ru^{II}(py)_4(NO^\bullet)]^{2+}$. The inertness of the latter species toward $NO^\bullet$ dissociation is remarkable. We also observed the same behavior for the $[RuCl(py)_4NO^\bullet]^+$ ion, consistently with the reported result for the $[Ru(bpy)_2ClNO^\bullet]^+$ ion.[19a] In contrast, cyanide or NO is rapidly released from $[Fe(CN)_5NO^\bullet]^{3-}$ [10] or from some members of the *trans*-$[Ru(NH_3)_4LNO]^{n+}$ series ensuing nitrosyl reduction (L = *N*-heterocyclic ligands, imidazole, H_2O, etc.), respectively.[22]

One-electron oxidation of **I** in AcN leads to $\mathbf{I_{ox}}$, whose IR spectrum in solution (Figure 3b) displays ν_{CN} stretching frequencies (see Table 1) characteristic of coordination to Ru(III).[21] The strong signal at 1952 cm^{-1}, ascribed to ν_{NO}, suggests that the $Ru^{II}-NO^+$ fragment is preserved upon oxidation, and that $\mathbf{I_{ox}}$ should be formulated as $[NCRu^{III}(py)_4(CN)Ru^{II}(py)_4(NO)]^{4+}$. The increase of ν_{NO} if compared to **I** probably reflects the electron-withdrawing influence of the distant Ru(III) center (see later).

The three redox-related species display a rich UV$-$vis spectroscopy (Figure 2, Table 1). Most of the features can be explained as a superposition of the electronic transitions of the two constituent $\{Ru(py)_4\}$ fragments, slightly perturbed by their mutual presence. Thus, **I** displays an intense band at 330 nm and a shoulder at 256 nm in AcN solution, which can be assigned to $d_\pi \rightarrow \pi^*_{py}$ and $\pi_{py} \rightarrow \pi^*_{py}$ transitions, respectively, within the dicyano chromophore. The intense peak at 237 nm can be assigned to the $d_\pi \rightarrow \pi^*_{py}$ transition in the $[Ru(py)_4NO]$ chromophore (see Table 1 for comparisons with the $[RuCl(py)_4NO]^{2+}$ complex). The fast decomposition of **I** upon irradiation in the 300$-$350 nm region is consistent with the absorption at the $Ru^{II}-$py chromophores, which could be followed by fast population of lower-lying d$-$d states and consequent labilization of pyridines. In the same spectral region, $\mathbf{I_{red}}$ displays two absorptions at 350 and 290 nm, probably also $d_\pi \rightarrow \pi^*_{py}$ in origin, corresponding to the dicyano- and NO-containing chromophores, respectively. Both absorptions are red-shifted compared to the similar transitions in **I**, as expected from the strong stabilization of the metal orbitals in **I** associated with the presence of the NO^+ ligand. Conversely, $\mathbf{I_{ox}}$ displays a series of characteristic LMCT transitions from cyanide to Ru(III),[23] in addition to the $\pi_{py} \rightarrow \pi^*_{py}$ transition appearing at greater wavelengths.

Strikingly, solutions of **I** are *deeply* violet colored in AcN because of a broad, intense band centered at 555 nm (Figure 2). This is remarkable, because the $[RuCl(py)_4NO]^{2+}$ ion[5] and many other mononuclear $[X_5M^{II}-(NO^+)]$ complexes (M = Fe, Ru, Os; X = cyanides, ammines, polypyridines) show *weak* bands in the visible region, which despite the low intensity have been assigned as Ru(II) $\rightarrow NO^+$ charge transfer (CT) transitions.[24] Under C_4 symmetry, the d_π orbitals of both metal centers transform as b and e. Only the latter have the appropriate symmetry to interact with the empty π^* orbitals in the isoelectronic CN^- and NO^+ fragments. The orbital interaction might result in extended MOs that provide the pathway for long-range electronic communication. Following this idea, we assign the intense visible band to a symmetry allowed transition between orbitals of e symmetry,[25] which involves a $d_{\pi(Ru^{II}\ distant)} \rightarrow \pi^*_{(\{Ru-NO\}^6)}$ charge transfer.

The following additional evidence supports our interpretation: (1) The visible band disappears upon reduction of NO^+ or oxidation of the distant Ru(II), as shown in Figure 2. (2)

(19) (a) Callahan, R. W.; Meyer, T. J. *Inorg. Chem.* **1977**, *16*, 574. (b) Abruña, H. D.; Walsh, J. L.; Meyer, T. J.; Murray, R. W. *J. Am. Chem. Soc.* **1980**, *102*, 3272.

(20) Baumann, F.; Kaim, W.; Baraldo, L. M.; Slep, L. D.; Olabe, J. A.; Fiedler, J. *Inorg. Chim. Acta* **1999**, *285*, 129.

(21) Nakamoto, K. *Infrared and Raman Spectra of Inorganic and Coordination Compounds*, 4th ed.; Wiley: New York, 1986.

(22) (a) Gomes, M. G.; Davanzo, C. U.; Silva, S. C.; Lopes, L. G. F.; Santos, P. S.; Franco, D. W. *J. Chem. Soc., Dalton Trans.* **1998**, 601. (b) Borges, S. da S. S.; Davanzo, C. U.; Castellano, E. E.; Z-Schpector, J.; Silva, S. S.; Franco, D. W. *Inorg. Chem.* **1998**, *37*, 2670.

(23) Kang, H. W.; Moran, G.; Krausz, E. *Inorg. Chim. Acta* **1996**, *249*, 231.

(24) Gorelsky, S. I.; da Silva, S. C.; Lever, A. B. P.; Franco, D. W. *Inorg. Chim. Acta* **2000**, *300*$-$*302*, 698 and references therein.

(25) Though b $\rightarrow$ e transitions are not symmetry-forbidden, they are expected to contribute with very low intensity to the spectrum because of poor overlap between the orbitals involved.

The solvatochromic behavior is compatible with the terminal cyanide on the donor fragment behaving as an electron donor toward the solvent.[26] The interaction with acceptor solvents contributes to stabilize the e(d_π) orbitals in the donor fragment. The $\{Ru-NO\}^6$ moiety is less sensitive to the solvent; consequently, the CT band shifts to higher energy in high acceptor number solvents.[27] (3) The RR experiment shows enhancement of ν_{CN} and ν_{NO}. Although both terminal and bridging cyanides (ν_{CNt} and ν_{CNbr}, respectively) could be coupled to the electronic transition,[3d,28] we propose that the great Raman intensity at 2000 cm^{-1} arises from ν_{CNbr}, in agreement with RR results in cyano-bridged mixed-valent complexes (see also later on the IR "red-shift" of ν_{CNbr}, compared to ν_{CNt} in the latter systems).[2b] (4) Preliminary experiments show that selective irradiation of the visible band induces the release of NO. A detailed photochemical study has not been performed, but similar results have been reported for $[Fe(CN)_5NO]^{2-}$,[29] *cis*-$[Ru^{II}(bpy)_2Cl(NO)]^{2+}$,[19a] and *trans*-$[Ru^{II}(NH_3)_4L(NO)]^{3+}$ complexes (L = py, pz and derivatives).[22] The proposed mechanism relies on the CT assignment of the absorption bands. Compound **I** is quite stable under exposure to diffuse daylight (in contrast to other nitrosyl containing substances such as $[Fe(CN)_5NO]^{2-}$), suggesting that the quantum efficiency of the photoprocess is low.

Remarkably, both ν_{CN} and ν_{NO} in **I** are solvent-dependent. The greater values of ν_{CN} and ν_{NO} in water compared to those in AcN are consistent with the decrease in electronic density in the donor fragment due to a greater interaction of the exposed cyanide with water (see previous discussion).

Role of Donor−Acceptor (D/A) Coupling. Long-range CT bands may arise from donor/acceptor (D/A) interactions between (covalently) linked fragments. In this context, the low energy band in **I** can be viewed as a D → A transition between the distant Ru(II) donor and the $\{Ru-NO\}^6$ acceptor (DACT).

The *energy* of the DACT is related to the redox potentials at the donor and acceptor sites, according to

$$h\nu = \Delta E_{redox} + \chi_i + \chi_o + C \qquad (2)$$

In eq 2, $h\nu$ is the energy of the optical transition in **I** (2.23 eV), ΔE_{redox} is the difference of redox potentials at the donor and acceptor sites (0.90 V), χ_i and χ_o are the reorganization energy parameters for the CT process, and C includes solvational energy contributions.[30,31] The difference between $h\nu$ and ΔE_{redox} is, in our case, 1.33 eV, a large value if compared to other D/A systems, as the related mixed-valent ion, $[Cl(py)_4Ru^{III}(NC)Ru^{II}(py)_4CN]^{2+}$ (ΔE_{redox} = 0.67 V; $h\nu$ = 1.38 eV; and ($h\nu - \Delta E_{redox}$) = 0.71 eV).[32] This could be traced to the changes in reorganization energies, provided that the Ru−N and N−O distances are known to change upon reduction, while the Ru−N−O fragment bends,[18] in contrast to the small distance changes expected to occur within the $Ru^{II,III}$ redox centers.[33,34]

The *oscillator strength* of the DACT is a function of the D/A coupling. The high intensity observed for **I** is indicative of efficient long-range electronic communication along the axial π-backbone. Estimation of the electronic coupling can be achieved using the Born−Oppenheimer aproximation and first-order perturbation theory arguments (Marcus−Hush formalism).[35] The D/A interaction is then described in terms of H_{DA}, the off-diagonal electronic coupling matrix element, which can be estimated from the experimental absorption band as

$$H_{DA} = (0.0205/r_{DA})[\epsilon_{max}\Delta\nu_{1/2}\nu_{max}]^{1/2} \qquad (3)$$

In eq 3, ϵ_{max}, $\Delta\nu_{1/2}$, and ν_{max} are the extinction coefficient, the full width at half-height, and the wavenumber of the DACT at its absorption maximum, respectively. r_{DA} is the transition dipole length, that is, the effective one-electron transfer distance, and the DACT band shape is assumed to be Gaussian. The values for the previously mentioned band properties of **I** are 5.8×10^3, 5.6×10^3, and 1.8×10^4 cm^{-1}, respectively. If r_{DA} is approximated to the distance between the Ru bound to the C of the cyano bridge and the N of nitrosyl (r_{DA} = 6.98 Å),[36] H_{DA} is ∼2200 cm^{-1}. This is in very good agreement with reported values for dinuclear cyano-bridged mixed-valent compounds.[37] On the other hand, assuming that the charge is transferred between the two ruthenium sites (r_{DA} = 5.21 A), we calculate an anomalous great value for H_{DA}, ∼3000 cm^{-1}. Eventually, a more precise value of the D/A distance is required to fully understand the electronic properties of this complex. Despite these uncertainties, the intensity of the DACT suggests a moderate to strong D/A coupling.

The IR spectral data for **I** (Table 1) show unusual low numbers for ν_{CN}. We assign the band at 2001 cm^{-1} (in AcN)

(26) Timpson, C. J.; Bignozzi, C. A.; Sullivan, B. P.; Kober, E. M.; Meyer, T. J. *J. Phys. Chem.* **1996**, *100*, 2915.
(27) Actually, the magnitude of the shift is comparable to that observed in the CT transitions of related compounds containing *one* cyanide.[26]
(28) (a) Bignozzi, C. A.; Argazzi, R.; Schoonover, J. R.; Gordon, K. C.; Dyer, R. B.; Scandola, F. *Inorg. Chem.* **1992**, *31*, 5260. (b) Forlano, P.; Baraldo, L. M.; Olabe, J. A.; Della Védova, C. O. *Inorg. Chim. Acta* **1994**, *223*, 37.
(29) Wolfe, S. K.; Swinehart, J. H. *Inorg. Chem.* **1975**, *14*, 1049.
(30) Lever, A. B. P.; Dodsworth, E. S. In *Inorganic Electronic Structure and Spectroscopy*; Solomon, E. I., Lever, A. B. P., Eds.; Wiley: New York, 1999; Vol. II, p 227.
(31) Equation 2 allows us to correlate spectroscopic and electrochemical data, provided that several conditions are met, namely, that the CT bands have a Gaussian shape and that the donor and acceptor orbitals associated with the electronic transition are the same as those involved in the electrochemical processes. Configurational interactions mixing the ground and excited states are neglected. Solvational contributions to the *C* values could be around 0.1−0.3 eV (see ref 30 for details).
(32) Our experiments show that the $[Cl(py)_4Ru^{II}(NC)Ru^{II}(py)_4CN]^+$ ion[7] can be oxidized to $[ClRu^{III}(py)_4(NC)Ru^{II}(py)_4CN]^{2+}$. The latter compound shows a band at ∼900 nm, which may be assigned to the intervalence CT transition. Similar results were calculated by using data for the $[NCRu^{II}(py)_4(CN)Ru^{III}(NH_3)_5]^{3+}$ ion:[2c] ΔE_{redox} = 1.0 V.; $h\nu$ = 1.66 eV, and ($h\nu - \Delta E_{redox}$) = 0.66 eV.
(33) Creutz, C. *Prog. Inorg. Chem.* **1983**, *30*, 1.
(34) The orbitals involved in the CT process could be different from those involved in the redox processes. This factor could contribute to the observed ($h\nu - \Delta E_{redox}$) value, but it is not probably the origin of the large difference observed upon variation of the acceptor site.
(35) (a) Hush, N. S. *Prog. Inorg. Chem.* **1967**, *8*, 391. (b) Marcus, R. A.; Sutin, N. *Biochim. Biophys. Acta* **1985**, *811*, 265.
(36) The value for r_{DA} = 6.98 Å was estimated from data for the trinuclear *trans*-$[Cl(py)_4Ru(NC)Ru(py)_4(CN)Ru(py)_4Cl]^{2+}$ ion[7] (Ru−C, 2.04 Å; C−N, 1.16 Å; Ru−N(nitrile), 2.01 Å) and for the $[RuCl(py)_4NO]^{2+}$ ion (Ru−N (nitrosyl), 1.77 Å).[6b]
(37) (a) Burewicz, A.; Haim, A. *Inorg. Chem.* **1988**, *27*, 1611. (b) Díaz, C.; Arancibia, A. *Inorg. Chim. Acta* **1998**, *269*, 246.

to the stretching mode of the bridging cyanide, ν_{CNbr}, and we assign the very weak absorption at 2050 cm^{-1} to the terminal mode, ν_{CNt}, in consistency with the RR assignment. The weak band at 1976 cm^{-1} is probably related to a $^{13}C-N$ stretching. In $[Ru^{II}(CN)_2(py)_4]$, ν_{CN} was found at 2062 cm^{-1}.[5] A single value at 2064 cm^{-1} was also found in the *trans*-$[Cl(py)_4Ru^{II}(NC)Ru^{II}(py)_4CN]PF_6$ complex and was assigned to ν_{CNt} (ν_{CNbr} was claimed to be obscured by its low intensity, associated with a small dipolar change).[7] Although an increase was observed for ν_{CNbr} compared to ν_{CNt},[38] it has been suggested that back-bonding effects may contribute to a decrease in ν_{CNbr}.[28] Besides, in some mixed-valent systems such as $[NCRu^{II}(py)_4(CN)Ru^{III}(NH_3)_5]^{3+}$, the combination of a low value for ν_{CNbr} (2006 cm^{-1}) and a high intensity of the intervalence CT transition has been traced to electronic coupling between the metal centers.[2b,c]

Electrophilic Reactivity of I. The spectral changes shown in Figure 5 are consistent with reaction 1 (see the results section). The decay of the CT band of **I** is accompanied by a shift to lower energy and an increase of the absorption intensity of the bands associated with the $Ru^{II}-py$ chromophores (which probably include the new MLCT absorption to the nitro ligand). The SWV results at pH 9.4 show the expected two waves corresponding to the ruthenium centers; the wave at lower potential, 0.82 V, corresponds to oxidation at the fragment containing the nitro ligand (no reduction wave of the nitrosyl ligand is observed). On the other hand, the band at 1.2 V is still at a greater potential than that for $[Ru(CN)_2(py)_4]$, although smaller than for **I**, consistent with the weaker acceptor ability of the nitro ligand compared to NO^+. The value of K_1, 3.1×10^{15} M^{-2}, is smaller than the value measured for the similar reaction with $[Ru(trpy)(bpy)NO]^{3+}$, 2.1×10^{23} M^{-2}.[19b] Although the charges are the same, this is probably related to the greater E value for nitrosyl reduction in the latter complex, 0.25 V.[39]

The rate law can be interpreted on the basis of a generally accepted mechanism for the OH^- additions to nitrosyl complexes,[12] involving a slow reaction of OH^- to form the NO_2H ligand, and subsequent fast deprotonation. The rate constants, k_1 (M^{-1} s^{-1}), are the appropriate indicators of nucleophilic reactivity, rather than the frequently used equilibrium constants K_1 corresponding to the overall reaction.[12] The only values of k_1 available in the literature for the addition of OH^- correspond to the reactions of the pentacyanonitrosyl complexes. These are always lower than 1 M^{-1} s^{-1} at 25 °C.[40] The presently reported value, $k_1 = 9.2 \times 10^3$ M^{-1} s^{-1}, is the first one for a positively charged electrophile. The significant increase in k_1 can be traced to charge effects, or, more probably, to an increase in the redox potential for nitrosyl reduction; for instance, the potential for NO^+ reduction in the $[Ru(CN)_5NO]^{2-}$ ion is -0.39 V in aqueous solution,[41] compared to 0.22 V for complex **I**. In contrast, the values of ν_{NO} are strikingly similar for the described compounds (1926[40] and 1917 cm^{-1}, respectively, in KBr disk) and behave in the opposite sense as expected.[12b] Therefore, the increase in electrophilicity associated with an increase in ν_{NO} must be considered with caution when comparing values for a limited set of data. Clearly, additional measurements of k_1 values with a broader set of complexes are required,[39] and these data should be carefully analyzed by considering all three potentially significant variables, namely, the charges of the reactants, ν_{NO}, and the redox potentials at the nitrosyl site.

Activation parameters for reaction 1 show that $\Delta H^{\ddagger}$ is in the range usually obtained for other nitrosyl complexes (50−90 kJ mol^{-1}).[40] However, the high positive value of $\Delta S^{\ddagger}$, 135 J K^{-1} mol^{-1}, appears as remarkable, probably reflecting a strong desolvation when going to the transition state (adduct formation). This is in expected contrast with the negative entropies found for the reaction of OH^- with negatively charged electrophiles, such as the $[M(CN)_5NO]^{2-}$ ions (M = Fe, Ru, Os).[40]

The results in Figure 6 show that $\mathbf{I_{ox}}$ is unstable above pH 2. We suggest that $\mathbf{I_{ox}}$ is susceptible of nucleophilic attack, eq 4:

$$[NCRu^{III}(py)_4(CN)Ru^{II}(py)_4NO]^{4+} + 2OH^- \leftrightarrow [NCRu^{III}(py)_4(CN)Ru^{II}(py)_4NO_2]^{2+} + H_2O \quad (4)$$

Reaction 4 is followed by a complex set of irreversible reactions. It is feasible that $[NCRu^{III}(py)_4(CN)Ru^{II}(py)_4NO_2]^{2+}$ isomerizes to the stable form $[NCRu^{II}(py)_4(CN)Ru^{III}(py)_4NO_2]^{2+}$ and reacts further at the electrode producing $[NCRu^{III}(py)_4(CN)Ru^{III}(py)_4NO_2]^{3+}$. Given the known reactivity of the $Ru(III)-NO_2^-$ complexes,[42] the latter product should be unstable toward the disproportionation of NO_2^-, explaining the irreversible character of the oxidation.

The analysis of the electrochemical results at different pHs suggests that reaction 4 should attain 50% conversion around pH 3.0. Thus, we estimate that the equilibrium constant, K_4, is around 10^{22} M^{-2}, which is significantly greater than K_1. This suggests that an increase of electrophilicity at the nitrosyl ligand is also operative upon oxidation of the distant ruthenium center,[43] which is consistent with the previously discussed spectroscopic changes upon formation of $\mathbf{I_{ox}}$.

Conclusions

A new cyano-bridged complex with *trans* geometry, $[NC(py)_4Ru(CN)Ru(py)_4NO](PF_6)_3$, has been prepared, containing the nitrosyl (NO^+) ligand bound to one of the ruthenium(II) metal centers. A strong donor−acceptor interaction is established between both metal sites, as shown by an intense electronic band in the visible region, which can be analyzed

(38) Dows, D. A.; Haim, A.; Wilmarth, W. K. *J. Inorg. Nucl. Chem.* **1961**, *21*, 33.
(39) Roncaroli, F.; Ruggiero, M.; Franco, D. F.; Olabe, J. A. Work in progress.
(40) Baraldo, L. M.; Bessega, M. S.; Rigotti, G. E.; Olabe, J. A. *Inorg. Chem.* **1994**, *33*, 5890.
(41) Fiedler, J. *Collect. Czech. Chem. Commun.* **1993**, *58*, 461.
(42) Keene, R.; Salmon, D. J.; Walsh, J. L.; Abruña, H. D.; Meyer, T. J. *Inorg. Chem.* **1980**, *19*, 1896.
(43) We assume a positive correlation between the nucleophilic rate constants and the equilibrium constants for the addition reactions, as found with the pentacyanometalate systems (ref 40).

in terms of the Hush model, as with related mixed-valent systems. The coupled $\{Ru^{II}-NO^{+}\}_6$ site is the acceptor component of the charge transfer originated in the remote Ru(II)−donor fragment, with a significant participation of the π^* nitrosyl orbital as acceptor. The latter is also the site of electrophilic reactivity, as well as of chemical, electrochemical, or photoinduced reduction. The complex can also be oxidized at the $[NCRu(py)_4CN]$ fragment, thus increasing significantly the reactivity at the distant nitrosyl site. Specific interactions of the exposed cyanide with solvents of different acceptor number (water, AcN) show up in measurable spectroscopic changes. This anticipates the possibility of synthesizing new trinuclear, *trans* bridging units through the coordination of appropriate donor fragments. Thus, a controlled tuning of the reactivity at the nitrosyl site can be envisaged, which could also be achieved by the introduction of appropriate substituents at the pyridine ligands.

Acknowledgment. We thank the University of Buenos Aires, the National Scientific Council (CONICET), the Agency for Science Promotion (ANPCYT), and the Volkswagenstiftung for financial support. J.A.O. and L.M.B. are members of the scientific staff, and L.D.S. and F.R. are postgraduate and graduate fellows from CONICET, respectively. We thank Prof. K. Wieghardt (Max-Planck-Institut für Strahlenchemie) for providing access to his laboratory equipment, to Daniel Murgida for the Raman measurements, and to E. Bill and T. Weyhermüller for many discussions and suggestions.

IC0109896